Nonlinear Dyn (2017) 88:465–476
DOI 10.1007/s11071-016-3253-8

REVIEW

Nonlinear disturbance observer-based backstepping finite-time sliding mode tracking control of underwater vehicles with system uncertainties and external disturbances

Siyuan Liu · Yancheng Liu · Ning Wang

Received: 7 July 2016 / Accepted: 24 November 2016 / Published online: 17 December 2016

Abstract In this paper, a nonlinear disturbance observer-based backstepping finite-time sliding mode control scheme for trajectory tracking of underwater vehicles subject to unknown system uncertainties and time-varying external disturbances is proposed. To reduce the influence of the uncertainties and external disturbances, a nonlinear disturbance observer is developed without any acceleration measurements to identify the lumped disturbance term. Additionally, the finite-time trajectory tracking controller is designed by combining second-order sliding mode control and backstepping design technique with the nonlinear disturbance observer. The finite-time convergence of motion tracking errors and the stability of the overall closed-loop control system are guaranteed by the Lyapunov approach. Besides, comprehensive simulation studies on trajectory tracking control of underwater vehicles are provided to demonstrate the effectiveness and performance of the proposed control scheme.

Keywords Underwater vehicles · Nonlinear disturbance observer · Sliding mode control · Backstepping technique · Finite-time convergence

S. Liu (✉) · Y. Liu (✉) · N. Wang
Marine Engineering College, Dalian Maritime University, Dalian 116026, China
e-mail: dmu.s.y.liu@gmail.com

Y. Liu
e-mail: liuyc3@126.com

N. Wang
e-mail: n.wang.dmu.cn@gmail.com

1 Introduction

Underwater vehicles are self-energizing and self-propelled intelligent equipments with autonomous controllers and various sensors, where the efficient and reliable autonomous controllers are highly desired for different types of underwater missions. Thus, a great deal of attentions have been paid to the accurate trajectory tracking (TT) control of underwater vehicles, which provides the fundamental technical support for various dynamic and complex missions, mainly because of the great practical significance for marine traffic safety. Commonly in practical situation, underwater vehicles are always coupled and highly nonlinear subject to diverse external disturbances that adversely affect performance, and the system parameters of underwater vehicles may not be known exactly; therefore, the design of TT controller of underwater vehicles is quite challenging and difficult.

To achieve high-precision tracking performance, a large variety of motion tracking control schemes of underwater vehicles have been proposed in the literatures for solving the TT control problem of underwater vehicles, which includes adaptive control [1–3], backstepping design technique [4–6], sliding mode control (SMC) [7–11], LMI-based control [12], fuzzy logic system [13–16], neural network control [17–20] and fuzzy neural network [21–25]. Among these methods, SMC has been shown to be a potentially useful approach when applied to a system subject to disturbances which satisfies the matched uncertainty condition. Moreover, SMC can offer many good properties, such as insensitivity to system uncertainties, disturbance rejection and fast dynamic response. However, the SMC-based motion controllers of underwater vehicles proposed in [7–11] are designed based on an asymptotic stability analysis which implies that the system trajectories converge to the equilibrium with infinite settling time. Therefore, a faster convergence to the required orientation in finite time is highly desired. Fortunately, the finite-time stabilization of dynamic systems may provide not only faster convergence but also better disturbance attenuation. The terminal sliding mode control (TSMC) [26,27] is a representative method used to design a robust controller which can guarantee a finite-time convergence to the origin. Another advanced sliding mode, namely the second-order SMC (SOSMC), which preserves the robustness ability of SMC and also yields improved accuracy and performance, has been paid attention in many literatures [28–30]. Although SOSMC controller is less sensitive to parameter uncertainties and external disturbances, its robustness is normally obtained by a large switching gain which causes the undesired chattering phenomenon. To alleviate above drawbacks, recently, the backstepping design technique is combined with sliding mode control to relax the matching condition at the expense of a high feedback gain required for robustness [31].

On the other hand, the system uncertainties and external disturbance are always unknown and nonlinear; thus, it is necessary to employ some disturbance suppression or attenuation methods to achieve the desired robust performance. Despite of above methods, an alternative emerged in recent years is the use of so-called disturbance observers control (DOBC). Roughly stated, the essence of the DOBC is to lump all internal uncertainties and external unknown disturbances acting on the underwater vehicles into a single term and then identify the unknown lumped term with the disturbance observer. It is found that the disturbance observers can provide fast, excellent tracking performance and smooth control actions without the use of large feedback gains such that the robustness of controller can be improved [32–37]. A nonlinear disturbance observer was proposed in [32] to handle nonlinear systems with disturbances, which is applied to tracking control of pneumatic artificial muscle actuator using dynamic surface control (DSC) scheme [33]. A new type of composite control scheme for the uncertain structural systems was proposed in [34], which combines the disturbance observer-based control and the TSMC. Yang et al. [35] investigated a sliding mode control for nonlinear systems with mismatched uncertainties by the use of a disturbance observer. In the design process of above disturbance observers, it is assumed to vary slowly relative to the observer dynamics, namely, the derivative of disturbance is approximately equal to zero. However, in practice, the external disturbance usually varies in a complex way due to the ocean currents and waves, and its change rate is always bounded in the specific mission environment. Bu et al. [36] proposed a new nonlinear disturbance observer (NDO) based on tracking differentiator, which can be used to estimate many types of uncertain disturbances, and can overcome the disadvantages of existing NDOs that need the *priori* information concerning the upper and lower bounds of the disturbance and its ith derivatives Lipschitz upper bound. In [37], a novel NDO is constructed using a new TD designed based on hyperbolic sine function to estimate the model uncertainties and varying disturbances.

In this paper, a novel nonlinear disturbance observer-based backstepping finite-time sliding mode control (NDOB-BFTSMC) scheme is proposed for trajectory tracking of underwater vehicles with system uncertainties and external disturbances. In the proposed NDOB-BFTSMC scheme, backstepping design technique and the second-order sliding mode control are integrated to preserve the advantages and alleviate the drawbacks of each method. Particularly, the finite-time stability of the closed-loop control system is guaranteed by this way. Under the framework of BFTSMC, to compensate the unknown system uncertainties and external disturbance and further relax the matching condition of exact model information, a nonlinear disturbance observer (NDOB) is developed for online identifying the lumped disturbance term accurately. The main contributions of the proposed control scheme are summarized as follows.

(1) A backstepping second-order sliding mode control framework is constructed for trajectory tracking control of underwater vehicles. To relax the matching condition at the expense of a larger switching gain of SOSMC, the backstepping design technique is combined with SOSMC such that a second-order sliding surface is defined in backstepping procedures, and the second-order sliding mode control law is designed to

guarantee the finite-time stability of the overall control system.

(2) Note that there exist unmodeled dynamics, parameter variations and unknown external disturbances in the underwater vehicle systems, then these uncertainties and disturbances are lumped into a single disturbance term. To online identify the lumped disturbance, a nonlinear disturbance observer is proposed without any acceleration measurements, which requires no knowledge of full dynamics such that further relax the matching condition at the expense of a larger switching gain on the basis of backstepping technique.

The remainder of this paper is organized as follows. The problem formulations and preliminaries are described in Sect. 2. The design of nonlinear disturbance observer and the proposed NDOB-BFTSMC are presented in Sect. 3. Moreover, the stability of the disturbance observer and overall closed-loop control system are also addressed in Sect. 3. The simulation studies are given in Sect. 4. Finally, the conclusion is drawn in Sect. 5.

2 Problem formulations and preliminaries

Consider the dynamics of an 5-DOF underwater vehicles in following form [38,39]:

$$\dot{\boldsymbol{\eta}} = \boldsymbol{J}(\boldsymbol{\eta})\boldsymbol{v} \tag{1a}$$

$$\boldsymbol{M}\dot{\boldsymbol{v}} + \boldsymbol{C}(\boldsymbol{v})\boldsymbol{v} + \boldsymbol{D}(\boldsymbol{v})\boldsymbol{v} + \boldsymbol{g}(\boldsymbol{\eta}) = \boldsymbol{\tau} + \boldsymbol{\tau}_{ex} \tag{1b}$$

where $\boldsymbol{\eta} = [x, y, z, \theta, \psi]^T$ is the positions and attitudes vector, $\boldsymbol{v} = [u, v, w, q, r]^T$ is the linear and angle velocities vector, $\boldsymbol{M} \in \mathbb{R}^{5\times5}$ is the inertia matrix, $\boldsymbol{C} \in \mathbb{R}^{5\times5}$ is the Coriolis and centrifugal matrix, $\boldsymbol{D} \in \mathbb{R}^{5\times5}$ is the drag forces (gravity) matrix, $\boldsymbol{g} \in \mathbb{R}^{5\times1}$ is the restoring forces (buoyancy) vector, $\boldsymbol{\tau} = [\tau_1, \tau_2, \tau_3, \tau_4, \tau_5]^T$ is the control torques vector applied to the underwater vehicles, $\boldsymbol{\tau}_{ex} = [\tau_{ex1}, \tau_{ex2}, \tau_{ex3}, \tau_{ex4}, \tau_{ex5}]^T$ is the time-varying unknown external disturbances vector due to ocean currents and waves, and $\boldsymbol{J}(\boldsymbol{\eta})$ is the rotation matrix defined as

$$\boldsymbol{J}(\boldsymbol{\eta}) = \begin{bmatrix} \cos\psi\cos\theta & -\sin\psi & \cos\psi\sin\theta & 0 & 0 \\ \sin\psi\cos\theta & \cos\psi & \sin\psi\sin\theta & 0 & 0 \\ -\sin\theta & 0 & \cos\theta & 0 & 0 \\ 0 & 0 & 0 & 1 & 0 \\ 0 & 0 & 0 & 0 & \frac{1}{\cos\theta} \end{bmatrix} \tag{2}$$

Underwater vehicles have several inherent dynamic properties, which are listed below and will be used for designing the extend disturbance observer later.

Property 1 *The inertia matrix $\boldsymbol{M}$ is symmetric positive definite and bounded, i.e., $\boldsymbol{M} = \boldsymbol{M}^T > 0$, $\varpi_{M_0} \leq \|\boldsymbol{M}\| \leq \varpi_{M_1}$. By using body symmetry conditions, i.e., $xz-$, $yz-$ and xy-planes of symmetry, the detailed expression of $\boldsymbol{M}$ is simplified as [39]*

$$\boldsymbol{M} = diag\{m_{11}, m_{22}, m_{33}, m_{44}, m_{55}\} \tag{3}$$

where ϖ_{M_0} and ϖ_{M_1} are unknown constants, $m_{11} = m - X_{\dot{u}}$, $m_{22} = m - Y_{\dot{v}}$, $m_{33} = m - Z_{\dot{w}}$, $m_{44} = I_y - M_{\dot{q}}$, $m_{55} = I_z - N_{\dot{r}}$. Here, m is the mass of the underwater vehicle, I_y and I_z are the moments of inertia about the pitch and yaw rotation, respectively, and X_*, Y_*, Z_*, M_* and N_* are the corresponding hydrodynamic derivatives.

Property 2 *The matrix $\dot{\boldsymbol{M}} - 2\boldsymbol{C}(\boldsymbol{v})$ is skew-symmetric [39], i.e.,*

$$[\dot{\boldsymbol{M}} - 2\boldsymbol{C}(\boldsymbol{v})]^T = -[\dot{\boldsymbol{M}} - 2\boldsymbol{C}(\boldsymbol{v})] \Rightarrow \dot{\boldsymbol{M}} = \boldsymbol{C}(\boldsymbol{v}) + \boldsymbol{C}^T(\boldsymbol{v}) \tag{4}$$

it follows that

$$\boldsymbol{v}^T[\dot{\boldsymbol{M}} - 2\boldsymbol{C}(\boldsymbol{v})]\boldsymbol{v} \equiv 0,\ \forall \boldsymbol{v} \in \mathbb{R}^{5\times1} \tag{5}$$

Here, the Coriolis and centrifugal matrix $\boldsymbol{C}(\boldsymbol{v})$ is given by

$$\boldsymbol{C}(\boldsymbol{v}) = \begin{bmatrix} 0 & 0 & 0 & c_{14} & c_{15} \\ 0 & 0 & 0 & 0 & c_{25} \\ 0 & 0 & 0 & c_{34} & 0 \\ c_{41} & 0 & c_{43} & 0 & 0 \\ c_{51} & c_{52} & 0 & 0 & 0 \end{bmatrix} \tag{6}$$

where $c_{14} = (m - Z_{\dot{w}})w$, $c_{15} = -(m - Y_{\dot{v}})v$, $c_{25} = (m - X_{\dot{u}})u$, $c_{34} = -(m - X_{\dot{u}})u$, $c_{41} = -(m - Z_{\dot{w}})w$, $c_{43} = (m - X_{\dot{u}})u$, $c_{51} = (m - Y_{\dot{v}})v$, $c_{52} = -(m - X_{\dot{u}})u$. Moreover, the drag force matrix and restoring force vector are given by

$$\boldsymbol{D}(\boldsymbol{v}) = \mathrm{diag}(d_{11}, d_{22}, d_{33}, d_{44}, d_{55}) \tag{7}$$

$$\boldsymbol{g}(\boldsymbol{\eta}) = [g_1, g_2, g_3, g_4, g_5]^T \tag{8}$$

where $d_{11} = -X_u - X_{|u|u}|u|$, $d_{22} = -Y_v - Y_{|v|v}|v|$, $d_{33} = -Z_w - Z_{|w|w}|w|$, $d_{44} = -M_q - M_{|q|q}|q|$, $d_{55} = -N_r - N_{|r|r}|r|$, $g_1 = (P - B)\sin\theta$, $g_2 = 0$, $g_3 =$

$-(P - B)\cos\theta$, $g_4 = -z_B B \sin\theta$, $g_5 = 0$. Here, P and B are the gravity and the buoyancy of underwater vehicles with center $\boldsymbol{r}_P$ and $\boldsymbol{r}_B$, respectively.

Now, by considering the additive uncertainties $\Delta *$, the parameters in (1b) can be defined as $\boldsymbol{C} = \boldsymbol{C}_0 + \Delta\boldsymbol{C}$, $\boldsymbol{D} = \boldsymbol{D}_0 + \Delta\boldsymbol{D}$, $\boldsymbol{g} = \boldsymbol{g}_0 + \Delta\boldsymbol{g}$. Then, the effect of unknown parameter uncertainties and external disturbances can be lumped into a disturbance vector $\boldsymbol{\tau}_d$. Therefore, the underwater vehicles dynamics (1) is rewritten as

$$\dot{\boldsymbol{\eta}} = \boldsymbol{J}(\boldsymbol{\eta})\boldsymbol{v} \tag{9a}$$

$$\dot{\boldsymbol{v}} = \boldsymbol{F}(\boldsymbol{v}, \boldsymbol{\eta}) + \boldsymbol{G}(\boldsymbol{\tau} + \boldsymbol{\tau}_d) \tag{9b}$$

where $\boldsymbol{F}(\boldsymbol{v}, \boldsymbol{\eta}) = -\boldsymbol{M}^{-1}(\boldsymbol{C}_0(\boldsymbol{v})\boldsymbol{v} + \boldsymbol{D}_0(\boldsymbol{v})\boldsymbol{v} + \boldsymbol{g}_0(\boldsymbol{\eta}))$, $\boldsymbol{G} = \boldsymbol{M}^{-1}$, $\boldsymbol{\tau}_d = \boldsymbol{\tau}_{ex} - \Delta\boldsymbol{C}(\boldsymbol{v})\boldsymbol{v} - \Delta\boldsymbol{D}(\boldsymbol{v}) - \Delta\boldsymbol{g}(\boldsymbol{\eta})$.

Lemma 1 *[40] Suppose that $V(\boldsymbol{x})$ is a smooth positive definite function (defined on $U \subset \mathbb{R}^n$) and $\dot{V}(\boldsymbol{x}) + \varrho V^{\varsigma}(\boldsymbol{x})$ is negative semi-definite on $U \subset \mathbb{R}^n$ for $\varsigma \in (0, 1)$ and $\varrho \in \mathbb{R}^+$, then there exists an area $U_0 \subset \mathbb{R}^n$ such that any $V(\boldsymbol{x})$ which starts from $U_0 \subset \mathbb{R}^n$ can reach $V(\boldsymbol{x}) \equiv 0$ in finite time. Moreover, if t_r is the time required to reach $V(\boldsymbol{x}) \equiv 0$ then*

$$t_r \leq \frac{V^{1-\varsigma}(\boldsymbol{x}_0)}{\varrho(1-\varsigma)} \tag{10}$$

where $V(\boldsymbol{x}_0)$ is the initial value of $V(\boldsymbol{x})$.

Lemma 2 *[41] For $\nu \in \mathbb{R}^+$ and $\varepsilon > 0$ it holds that*

$$0 < |v| - v\tanh(\varepsilon v) \leq \frac{0.2785}{\varepsilon} \tag{11}$$

The control objective of this paper is to design a nonlinear disturbance observer-based backstepping second-order sliding mode control scheme such that all signals in the overall closed-loop system are bounded, and the trajectory states can track the given reference trajectories in the presence of time-varying disturbances and system uncertainties. Moreover, the tracking errors and sliding surface converge to a invariant region in finite time.

3 Nonlinear disturbances observer-based backstepping finite-time sliding mode control

In this section, a nonlinear disturbance observer-based backstepping finite-time sliding mode controller (NDOB-BFTSMC) will be developed, where the nonlinear disturbance observer is proposed without any acceleration measurement to online identify the unknown time-varying disturbances, and then the control bandwidth and tracking precision are improved.

3.1 Nonlinear disturbance observer design

Acceleration measurements are usually available for underwater vehicles system, so the disturbances observer can take following form

$$\dot{\hat{\boldsymbol{\tau}}}_d = -\boldsymbol{L}\hat{\boldsymbol{\tau}}_d + \boldsymbol{L}(\boldsymbol{M}\dot{\boldsymbol{v}} + \boldsymbol{N}(\boldsymbol{\eta}, \boldsymbol{v}) - \boldsymbol{\tau}) \tag{12}$$

where

$$\boldsymbol{N}(\boldsymbol{\eta}, \boldsymbol{v}) = \boldsymbol{C}_0\boldsymbol{v} + \boldsymbol{D}_0\boldsymbol{v} + \boldsymbol{g}_0 \tag{13}$$

and $\boldsymbol{L} = \mathrm{diag}(l_1, \ldots, l_5)$ is the observer gain matrix, which is positive definite, i.e., $l_i > 0$, $i = 1, \ldots, 5$.

Note that the precision of above observer relies on that of acceleration measurements; however, high-accuracy accelerometers are not available for many underwater vehicles; thus, a nonlinear disturbance observer without any acceleration measurement is highly desired. Now, we introduce an auxiliary variable given as

$$\boldsymbol{\epsilon} = \hat{\boldsymbol{\tau}}_d - \boldsymbol{p}(\boldsymbol{v}) \tag{14}$$

where the auxiliary vector $\boldsymbol{p}(\boldsymbol{v})$ can be determined from the observer gain matrix as follows

$$\frac{\mathrm{d}}{\mathrm{d}t}\boldsymbol{p}(\boldsymbol{v}) = \boldsymbol{L}\boldsymbol{M}\dot{\boldsymbol{v}} \tag{15}$$

By taking the time derivative of (14) together with (12) yields

$$\begin{aligned}\dot{\boldsymbol{\epsilon}} &= \dot{\hat{\boldsymbol{\tau}}}_d - \dot{\boldsymbol{p}}(\dot{\boldsymbol{v}}) = \dot{\hat{\boldsymbol{\tau}}}_d - \boldsymbol{L}\boldsymbol{M}\dot{\boldsymbol{v}} \\ &= -\boldsymbol{L}(\boldsymbol{\epsilon} + \boldsymbol{p}) + \boldsymbol{L}(\boldsymbol{M}\dot{\boldsymbol{v}} + \boldsymbol{N}(\boldsymbol{\eta}, \boldsymbol{v}) - \boldsymbol{\tau} - \boldsymbol{M}\dot{\boldsymbol{v}}) \\ &= -\boldsymbol{L}\boldsymbol{\epsilon} + \boldsymbol{L}(\boldsymbol{N}(\boldsymbol{\eta}, \boldsymbol{v}) - \boldsymbol{\tau} - \boldsymbol{p})\end{aligned} \tag{16}$$

Combining (14)–(16) together, the nonlinear disturbance observer takes following form

$$\begin{aligned}\dot{\boldsymbol{\epsilon}} &= -\boldsymbol{L}\boldsymbol{\epsilon} + \boldsymbol{L}(\boldsymbol{N}(\boldsymbol{\eta}, \boldsymbol{v}) - \boldsymbol{\tau} - \boldsymbol{p}) \\ \dot{\boldsymbol{p}} &= \boldsymbol{L}\boldsymbol{M}\dot{\boldsymbol{v}} \\ \hat{\boldsymbol{\tau}}_d &= \boldsymbol{\epsilon} + \boldsymbol{p}(\boldsymbol{v})\end{aligned} \tag{17}$$

From (15), note that the proposed nonlinear disturbance observer designed in (15) has no requirement of acceleration measurement due to cancellation of the term $\boldsymbol{M}\dot{\boldsymbol{v}}$. Then, with (9) and (12)–(14), the error dynamics of observation $\dot{\tilde{\boldsymbol{\tau}}}_d$ can be obtained as

$$\begin{aligned}\dot{\tilde{\boldsymbol{\tau}}}_d &= \dot{\boldsymbol{\tau}}_d - \dot{\hat{\boldsymbol{\tau}}}_d = \dot{\boldsymbol{\tau}}_d - \dot{\boldsymbol{\epsilon}} - \frac{d}{dt}\boldsymbol{p}(\boldsymbol{v}) \\ &= \dot{\boldsymbol{\tau}}_d + \boldsymbol{L}(\hat{\boldsymbol{\tau}}_d - \boldsymbol{p}) - \boldsymbol{L}(\boldsymbol{\tau}_d - \boldsymbol{M}\dot{\boldsymbol{v}} - \boldsymbol{p}) - \boldsymbol{L}\boldsymbol{M}\dot{\boldsymbol{v}} \\ &= \dot{\boldsymbol{\tau}}_d - \boldsymbol{L}\tilde{\boldsymbol{\tau}}_d \end{aligned} \tag{18}$$

The following theorem addresses the case when the underwater vehicles are subject to complex disturbances with bounded change rate.

Theorem 1 *Consider the underwater vehicles subject to lumped disturbances described by (9), the disturbance observer is designed as (15) with the observation gain matrix* $\boldsymbol{L}$ *and the auxiliary vector* $\boldsymbol{p}(\boldsymbol{v})$. *Under the condition that the change rate of the lumped disturbance is bounded, i.e., there exists an unknown constant* $\varpi_d > 0$ *such that* $\|\dot{\boldsymbol{\tau}}_d\| \leq \varpi_d$ *for all* $t > 0$. *The disturbance tracking error* $\tilde{\boldsymbol{\tau}}_d$ *is globally uniformly ultimately bounded (GUUB) and can be made arbitrarily small.*

Proof Consider the following Lyapunov candidate function:

$$V_0(\tilde{\boldsymbol{\tau}}_d) = \frac{1}{2}\tilde{\boldsymbol{\tau}}_d^T \boldsymbol{Q}\tilde{\boldsymbol{\tau}}_d \tag{19}$$

where $\boldsymbol{Q}$ is a positive definite matrix satisfying $\|\boldsymbol{Q}\| \leq \varpi_Q$. From (16), taking the derivative of V_0, it is obtained that

$$\begin{aligned}\dot{V}_0 &= \tilde{\boldsymbol{\tau}}_d^T \boldsymbol{Q}\dot{\tilde{\boldsymbol{\tau}}}_d = \tilde{\boldsymbol{\tau}}_d^T \boldsymbol{Q}(\dot{\boldsymbol{\tau}}_d - \boldsymbol{L}\tilde{\boldsymbol{\tau}}_d) \\ &= -\boldsymbol{Q}\boldsymbol{L}\|\tilde{\boldsymbol{\tau}}_d\|^2 + \tilde{\boldsymbol{\tau}}_d^T \boldsymbol{Q}\dot{\boldsymbol{\tau}}_d \end{aligned} \tag{20}$$

Since $\|\dot{\tau}_d\| \leq \varpi_d$, one can obtain following inequality

$$\tilde{\boldsymbol{\tau}}_d^T \boldsymbol{Q}\dot{\boldsymbol{\tau}}_d \leq \|\tilde{\boldsymbol{\tau}}_d\|^2 + \|\boldsymbol{Q}\|^2\|\dot{\boldsymbol{\tau}}_d\|^2 \leq \|\tilde{\boldsymbol{\tau}}_d\|^2 + \varpi_Q^2\varpi_d^2 \tag{21}$$

By the inequality (19) and (41), it is observed that

$$\begin{aligned}\dot{V}_0 &\leq -(\lambda_{\min}(\boldsymbol{L}) - 1)\|\tilde{\boldsymbol{\tau}}_d\|^2 + \varpi_Q^2\varpi_d^2 \\ &\leq -\alpha_0 V_0 + \beta_0 \end{aligned} \tag{22}$$

where $\alpha_0 = \lambda_{\min}(\boldsymbol{L}) - 1$, $\beta_0 = \varpi_Q^2\varpi_d^2$. From (20), it can be seen that

$$0 \leq V_0(t) \leq \frac{\beta_0}{\alpha_0} + \left(V_0(0) - \frac{\beta_0}{\alpha_0}\right)\exp(-\alpha_0 t) \tag{23}$$

According to the uniform ultimate boundedness theorems [51] and (21), it implies that $V_0(t)$ and the disturbance tracking error $\tilde{\boldsymbol{\tau}}_d$ are GUUB, namely,

$$\begin{aligned}&\|\tilde{\boldsymbol{\tau}}_d\|^2 \leq \frac{2\beta_0}{\alpha_0} + 2\left(V_0(0) - \frac{\beta_0}{\alpha_0}\right)\exp(-\alpha_0 t) \\ &\Rightarrow \|\tilde{\boldsymbol{\tau}}_d\| \leq \sqrt{\frac{2\beta_0}{\alpha_0} + 2\left(V_0(0) - \frac{\beta_0}{\alpha_0}\right)\exp(-\alpha_0 t)} \end{aligned} \tag{24}$$

Thus, the convergence rate of the disturbance tracking error is α_0, and there exists a time constant $T_0 > 0$, for any $\mu_0 > \sqrt{2\beta_0/\alpha_0}$ such that $\|\tilde{\boldsymbol{\tau}}_d\| \leq \mu_0$, where the bound μ_0 can be made arbitrarily small since β_0/α_0 can be rendered arbitrarily small if parameter $\boldsymbol{L}$ is selected appropriately, namely, a large enough $\boldsymbol{L}$ can guarantee a arbitrarily small disturbance tracking error even in the case of fast-varying disturbance. From (18) and (24), it is concluded that $\dot{\tilde{\boldsymbol{\tau}}}_d$ is bounded, i.e., $\|\dot{\tilde{\boldsymbol{\tau}}}_d\| \leq \varpi_c$, where $\varpi_c > 0$ is an unknown constant. This concludes the proof. □

3.2 Design of NDOB-BFTSMC

Define the tracking error $\boldsymbol{e}_1 = [e_{11}, \ldots, e_{15}]^T$ as

$$\boldsymbol{e}_1(t) = \boldsymbol{\eta}(t) - \boldsymbol{\eta}_r(t) \tag{25}$$

where $\boldsymbol{\eta}_r(t)$ is the reference trajectory. From (9), let $\boldsymbol{v}$ be a virtual input given by

$$\boldsymbol{v} = \boldsymbol{J}^T\left(\dot{\boldsymbol{\eta}}_r - \boldsymbol{\phi}(\boldsymbol{\kappa}_\eta, \boldsymbol{e}_1)\right) = \boldsymbol{\alpha}(\boldsymbol{e}_1) \tag{26}$$

where $\boldsymbol{\phi}(\boldsymbol{\kappa}_\eta, \boldsymbol{e}_1) = \boldsymbol{\kappa}_\eta \tanh\left(\frac{\boldsymbol{e}_1}{\mu_\eta}\right)$. Here, $\boldsymbol{\kappa}_\eta = \mathrm{diag}(\kappa_{\eta 1}, \ldots, \kappa_{\eta 5}) > 0$, μ_η is a small positive scalar and $\tanh\left(\frac{\boldsymbol{e}_1}{\mu_\eta}\right) = [\tanh\left(\frac{e_{11}}{\mu_\eta}\right)\ \tanh\left(\frac{e_{12}}{\mu_\eta}\right) \tanh\left(\frac{e_{13}}{\mu_\eta}\right)\ \tanh\left(\frac{e_{14}}{\mu_\eta}\right)\ \tanh\left(\frac{e_{15}}{\mu_\eta}\right)]^T$.

Define the tracking error $\boldsymbol{e}_2 = [e_{21}, \ldots, e_{25}]^T$ as $\boldsymbol{e}_2 = \boldsymbol{v} - \boldsymbol{\alpha}$. Then, (9) can be rewritten as follows

$$\begin{cases}\dot{\boldsymbol{e}}_1 &= \boldsymbol{J}\boldsymbol{e}_2 - \boldsymbol{\kappa}_\eta \tanh\left(\frac{\boldsymbol{e}_1}{\mu_\eta}\right) \\ \dot{\boldsymbol{e}}_2 &= \boldsymbol{F} + \boldsymbol{G}(\boldsymbol{\tau} + \boldsymbol{\tau}_d) - \dot{\boldsymbol{\alpha}}(\boldsymbol{e}_1)\end{cases} \tag{27}$$

where $\dot{\boldsymbol{\phi}}(\boldsymbol{e}_1)$ in $\dot{\boldsymbol{\alpha}}(\boldsymbol{e}_1)$ is determined by

$$\dot{\boldsymbol{\phi}}(\boldsymbol{e}_1) = \mu_\eta^{-1}\mathrm{diag}\left(\kappa_{\eta i}\,\mathrm{sech}^2\left(\frac{e_{1i}}{\mu_\eta}\right)\right)\dot{\boldsymbol{e}}_1 \tag{28}$$

Then, select the tracking error $\boldsymbol{s}_1 = \boldsymbol{e}_2$ and its derivative $\boldsymbol{s}_2 = \dot{\boldsymbol{e}}_2$ as the sliding variables, such that the sliding surface $\boldsymbol{\sigma}$ can be defined in following form

$$\boldsymbol{\sigma} = \boldsymbol{s}_2 + \boldsymbol{\lambda}\boldsymbol{s}_1 + \boldsymbol{\gamma}\int_0^t (\boldsymbol{s}_2 + \boldsymbol{\lambda}\boldsymbol{s}_1)d\tau \tag{29}$$

where $\boldsymbol{\lambda} = \mathrm{diag}(\lambda_1, \ldots, \lambda_5)$ and $\boldsymbol{\gamma} = \mathrm{diag}(\gamma_1, \ldots, \gamma_5)$ are positive definite matrices.

Therefore, the NDOB-BFTSMC law is designed to drive the system trajectory onto the sliding surface as

$$\boldsymbol{\tau} = \boldsymbol{G}^{-1}(-\boldsymbol{F} + \dot{\boldsymbol{\alpha}} + \boldsymbol{\tau}_s) - \hat{\boldsymbol{\tau}}_d \tag{30}$$

where $\boldsymbol{\tau}_s$ is determined as

$$\dot{\boldsymbol{\tau}}_s = -\boldsymbol{\lambda}\boldsymbol{s}_2 - \boldsymbol{\rho}\mathrm{sgn}(\boldsymbol{\sigma}) - \boldsymbol{\gamma}(\boldsymbol{s}_2 + \boldsymbol{\lambda}\boldsymbol{s}_1) - \boldsymbol{K}\boldsymbol{\sigma} \tag{31}$$

Here, $\boldsymbol{\rho} = \mathrm{diag}(\rho_1, \ldots, \rho_5)$ and $\boldsymbol{K} = \mathrm{diag}(k_1, \ldots, k_5)$ are positive definite matrices.

From (27), and according to the above definition of sliding variables, the derivatives of $\boldsymbol{s}_1$ and $\boldsymbol{s}_2$ can be obtained as

$$\begin{cases}\dot{\boldsymbol{s}}_1 = \boldsymbol{s}_2 \\ \dot{\boldsymbol{s}}_2 = -\boldsymbol{\lambda}\boldsymbol{s}_2 - \boldsymbol{\rho}\mathrm{sgn}(\boldsymbol{\sigma}) - \boldsymbol{\gamma}(\boldsymbol{s}_2 + \boldsymbol{\lambda}\boldsymbol{s}_1) - \boldsymbol{K}\boldsymbol{\sigma} + \boldsymbol{G}\dot{\tilde{\boldsymbol{\tau}}}_d\end{cases} \tag{32}$$

and then the time derivative of the sliding surface is obtained as

$$\dot{\boldsymbol{\sigma}} = -\boldsymbol{\rho}\mathrm{sgn}(\boldsymbol{\sigma}) - \boldsymbol{K}\boldsymbol{\sigma} + \boldsymbol{G}\dot{\tilde{\boldsymbol{\tau}}}_d \tag{33}$$

Theorem 2 *Consider the system dynamics in (9), the virtual input $\boldsymbol{\alpha}$ in (26) and the control law $\boldsymbol{\tau}$ in (30) and (31), in finite time, the tracking errors $\boldsymbol{e}_1$ and $\boldsymbol{e}_2$ and the sliding surface $\boldsymbol{\sigma}$ of the underwater vehicle system converge to the region*

$$\|\boldsymbol{\chi}\| \le \frac{\varpi}{\overline{\phi}} \tag{34}$$

where $\boldsymbol{\chi} = [\frac{\boldsymbol{e}_1^T}{\sqrt{2}}\ \frac{\boldsymbol{\sigma}^T}{\sqrt{2}}]^T$, $\varpi = 1.9325\mu_\eta$ *and* $\overline{\phi} = \min(\sqrt{2}\overline{\kappa}_\eta, \sqrt{2}(\overline{\rho} - \varpi_c))$ *with* $\overline{\kappa}_\eta = \min(\kappa_{\eta i})$ *and* $\overline{\rho} = \min(\rho_i)$ $(i = 1, \ldots, 5)$.

Proof Substituting $\boldsymbol{\upsilon}$ defined in (26) into the first equation of (27), one can obtain

$$\dot{\boldsymbol{e}}_1 = -\boldsymbol{\kappa}_\eta \tanh\left(\frac{\boldsymbol{e}_1}{\mu_\eta}\right) \tag{35}$$

Consider the Lyapunov candidate function as

$$V_1 = \frac{1}{2}\boldsymbol{e}_1^T\boldsymbol{e}_1 = \frac{1}{2}\sum_{i=1}^5 e_{1i}^2 \tag{36}$$

Then from (35), differentiating (36) with respect to time as follows

$$\begin{aligned}\dot{V}_1 &= \boldsymbol{e}_1^T\dot{\boldsymbol{e}}_1 \\ &= -\boldsymbol{e}_1^T\boldsymbol{\kappa}_\eta \tanh\left(\frac{\boldsymbol{e}_1}{\mu_\eta}\right) \\ &= -\sum_{i=1}^5 \kappa_{\eta i}e_{1i}\tanh\left(\frac{e_{1i}}{\mu_\eta}\right)\end{aligned} \tag{37}$$

According to Lemma 2, it is obtained that $0 < |e_{1i}| \le e_{1i}\tanh(\frac{e_{1i}}{\mu_\eta}) + 0.2785\mu_\eta$ such that (37) can be rearranged as

$$\begin{aligned}\dot{V}_1 &\le -\sum_{i=1}^5 \kappa_{\eta i}\left(|e_{1i}| - 0.2785\mu_\eta\right) \\ &\le -\sum_{i=1}^5 \kappa_{\eta i}|e_{1i}| + 0.2785\sum_{i=1}^5 \mu_\eta \\ &\le -\sqrt{2}\overline{\kappa}_\eta\|\boldsymbol{e}_1\| + \varpi\end{aligned} \tag{38}$$

where $\overline{\kappa}_\eta = \min(\kappa_{\eta i})$, $i = 1, \ldots, 5$, and $\varpi = 1.3925\mu_\eta$.

From Lemma 1, if $\|\boldsymbol{e}_1\| > \frac{\varpi}{\sqrt{2}\overline{\kappa}_\eta}$, then the finite-time stability is still guaranteed, namely, when the state moves outside the region

$$\|\boldsymbol{e}_1\| \le \frac{\varpi}{\sqrt{2}\overline{\kappa}_\eta} \tag{39}$$

$\dot{V}_1 < 0$ is guaranteed. Hence, the states e_{1i} of equilibrium of the differential equation $\dot{e}_{1i} = \kappa_{\eta i}\tanh\left(\frac{e_{1i}}{\mu_\eta}\right)$ will converge to the region (38) in finite time.

Furthermore, consider following Lyapunov candidate function

$$V_2 = \boldsymbol{\chi}^T\boldsymbol{\chi} = V_1 + \frac{1}{2}\boldsymbol{\sigma}^T\boldsymbol{\sigma} \tag{40}$$

From (33), the time derivative of V_2 is obtained as

$$\begin{aligned}\dot{V}_2 &= \dot{V}_1 + \boldsymbol{\sigma}^T \dot{\boldsymbol{\sigma}} \\ &= \dot{V}_1 + \boldsymbol{\sigma}^T \big(- \boldsymbol{\rho}\text{sgn}(\boldsymbol{\sigma}) - \boldsymbol{K}\boldsymbol{\sigma} + \boldsymbol{G}\dot{\hat{\boldsymbol{\tau}}}_d \big) \\ &\leq - \sum_{i=1}^{5} \kappa_{\eta i} |e_{1i}| - \sum_{i=1}^{5} \rho_i |\sigma_i| + 0.2785 \sum_{i=1}^{5} \mu_\eta \\ &\quad + \sum_{i=1}^{5} |\sigma_i||G_i||\dot{\hat{\tau}}_{di}| \end{aligned} \tag{41}$$

From Theorem 1 and Property 1, it is obtained that $\|\dot{\hat{\boldsymbol{\tau}}}_d\| \leq \varpi_c$ and $\|\boldsymbol{G}\| \leq \varpi_{M_0}^{-1}$. Thus, (40) can be rewritten as

$$\begin{aligned}\dot{V}_2 &\leq - \overline{\kappa}_\eta \sum_{i=1}^{5} |e_{1i}| - \overline{\rho} \sum_{i=1}^{5} |\sigma_i| + \varpi_{M_0}^{-1} \sum_{i=1}^{5} \varpi_c |\sigma_i| + \varpi \\ &\leq - \overline{\kappa}_\eta \sum_{i=1}^{5} |e_{1i}| - \big(\overline{\rho} - \varpi_c\big) \sum_{i=1}^{5} |\sigma_i| + \varpi \\ &\leq - \min\big(\sqrt{2}\overline{\kappa}_\eta, \sqrt{2}(\overline{\rho} - \varpi_c)\big) \\ &\quad \left(\sum_{i=1}^{5} \left(\frac{|\sigma_i|}{\sqrt{2}} \right)^2 + \sum_{i=1}^{5} \left(\frac{|e_{1i}|}{\sqrt{2}} \right)^2 \right)^{1/2} + \varpi \\ &= - \overline{\phi} \|\boldsymbol{\chi}\| + \varpi \end{aligned} \tag{42}$$

where $\overline{\phi} = \min\big(\sqrt{2}\overline{\kappa}_\eta, \sqrt{2}(\overline{\rho} - \varpi_c)\big)$. Note that $\dot{V}_2 < 0$ if $\|\boldsymbol{\chi}\| > \varpi/\overline{\phi}$, namely, the decrease of V_2 finally forces the trajectories of the closed-loop system into $\|\boldsymbol{\chi}\| > \varpi/\overline{\phi}$. Thus, the trajectories of the closed-loop system are ultimately bounded as

$$\lim_{t \to \infty} \boldsymbol{\chi} \in \left(\|\boldsymbol{\chi}\| > \frac{\varpi}{\overline{\phi}} \right) \tag{43}$$

which is a small set containing the origin of the closed-loop system. Therefore, from Lemma 1, the state $\boldsymbol{\chi}$ will converge to the region

$$\|\boldsymbol{\chi}\| \leq \frac{\varpi}{\overline{\phi}} \tag{44}$$

in finite time. This implies that $\sigma_i = 0$ $(i = 1, 2, \ldots, 5)$, and it follows that s_i and $\dot{s}_i$ are both quite close to zero. This completes the proof. □

It is worth noting that the accuracy of tracking errors and the convergence time are determined by the values of the parameters $\boldsymbol{\kappa}_\eta$, $\boldsymbol{\rho}$ and μ_η, which can be made arbitrarily small by increasing the value of $\boldsymbol{\kappa}_\eta$ and $\boldsymbol{\rho}$ and decreasing the value of μ_η, namely, large enough $\boldsymbol{\kappa}_\eta$ and $\boldsymbol{\rho}$ as well small enough μ_η can make the tracking errors arbitrarily small such that the convergence performance is improved.

4 Simulation studies

In order to verify the effectiveness and superiority of the proposed NDOB-BFTSMC scheme, several simulations are conduct on the underwater vehicle developed by the research group at Tokyo University of Marine Science and Technology [42]. The nominal parameter values of (1) are employed as follows: the mass $m = 390kg$; the moments of inertia $I_y = 305.67kgm^2$ and $I_z = 305.67kgm^2$; the derivatives of the added mass $X_{\dot{u}} = -49.12$, $Y_{\dot{v}} = -311.52$, $Z_{\dot{w}} = -311.52$ and $N_r = -200$; the coefficients of the linear skin friction $X_u = -20$, $Y_v = -200$, $Z_w = -200$, $M_q = -200$ and $N_r = -200$; the coefficients of the quadratic drag $X_{|u|u} = -30$, $Y_{|v|v} = -300$, $Z_{|w|w} = -300$, $M_{|q|q} = -300$ and $N_{|r|r} = -300$; the center of the underwater vehicle $x_B = 0$, $y_B = 0$, $z_B = -0.15$. Moreover, the actual plant model in (9) is constructed under the following conditions: for parameter uncertainties, $\triangle\boldsymbol{C} = -0.2\boldsymbol{C}$, $\triangle\boldsymbol{D} = 0.2\boldsymbol{D}$, $\triangle\boldsymbol{g} = 0.1\boldsymbol{g}$; for external disturbances $\boldsymbol{\tau}_{ex}(t)$, the complex environment involving ocean currents and waves are governed by

$$\boldsymbol{\tau}_{ex}(t) = \begin{bmatrix} 3 + 5\sin(4t - \pi/3) \\ 2 + 3\cos(2t - \pi/6) \\ 4 + 7\sin(3t - \pi/4) \\ 5 + 2\cos(0.5t - \pi/4) \\ 2 + 2\sin(0.5t + \pi/6) \end{bmatrix} \tag{45}$$

For achieving the control objective of high-accuracy tracking, the reference trajectory $\boldsymbol{\eta}_r$ governed by

$$\boldsymbol{\eta}_r(t) = \begin{bmatrix} \sin(0.02t) \\ \cos(0.01t) \\ \sin(0.01t) + 2\cos(0.01t) \\ -0.1\cos(0.01t) + 0.2\sin(0.01t) \\ 0.1\cos(0.01t) - 0.1\sin(0.01t) \end{bmatrix} \tag{46}$$

Moreover, the initial conditions are set as follows: $\boldsymbol{\eta}(0) = [0(m), 1(m), 1.5(m), 0(rad), 0(rad)]^T$, and the design parameters associated with the BFTSMC

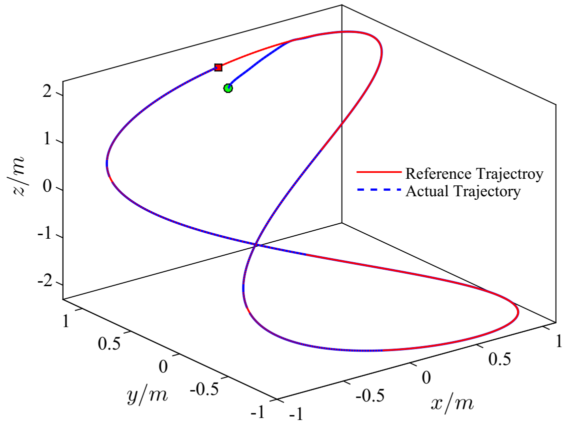

Fig. 1 Reference and actual trajectories in 3D presentation

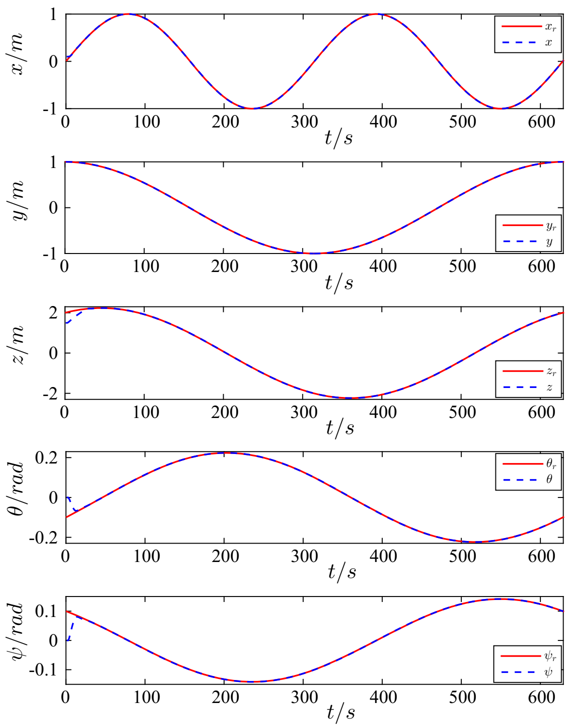

Fig. 2 Reference and actual trajectories in separate-dimension presentation

and NDOB are selected as follows: $\boldsymbol{\lambda} = \text{diag}(3, 3, 3, 3, 3)$, $\boldsymbol{\gamma} = \text{diag}(30, 30, 30, 30, 30)$, $\boldsymbol{K} = \text{diag}(30, 30, 30, 30, 30)$, $\boldsymbol{\kappa}_\eta = \text{diag}(2, 2, 2, 1.1, 1.1)$, $\boldsymbol{\rho} = \text{diag}(5, 5, 5, 5, 5)$, $\boldsymbol{L} = \text{diag}(80, 80, 80, 80, 80)$, $\mu_\eta = 0.05$.

The simulation results of reference and actual trajectories of tracking underwater vehicles are shown in Figs. 1 and 2, including the time history of the refer-

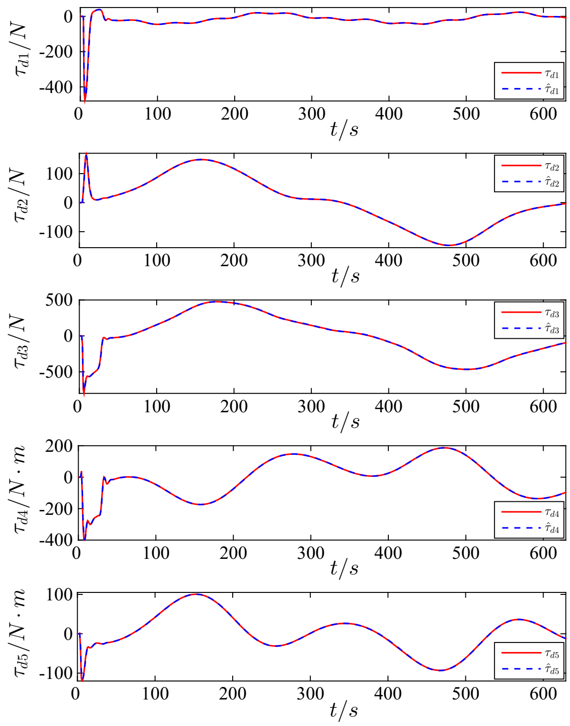

Fig. 3 Observation of the unknown lumped disturbance

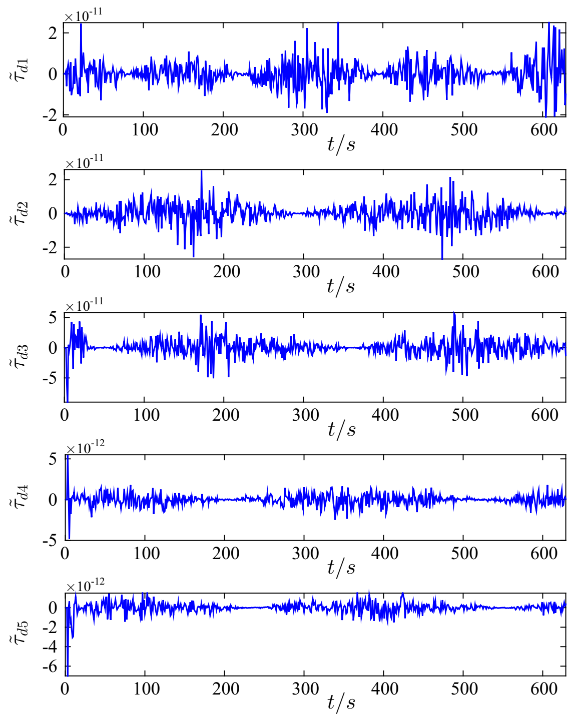

Fig. 4 Observation errors of unknown lumped disturbance

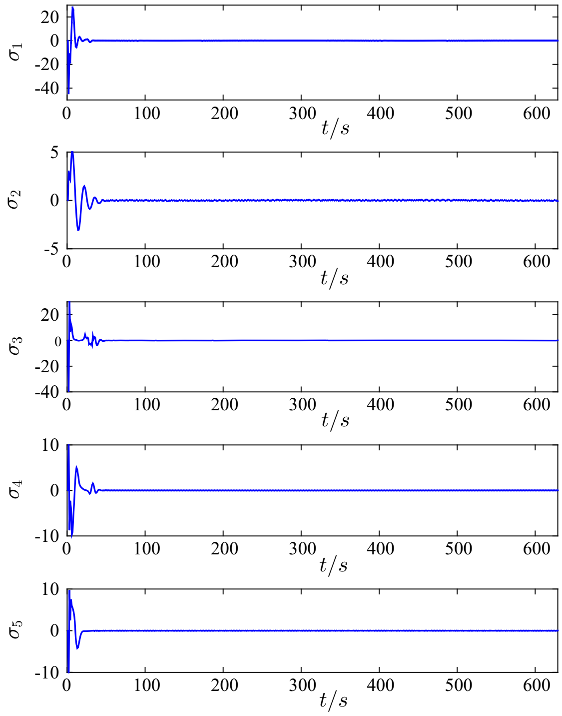

Fig. 5 Response of sliding surface

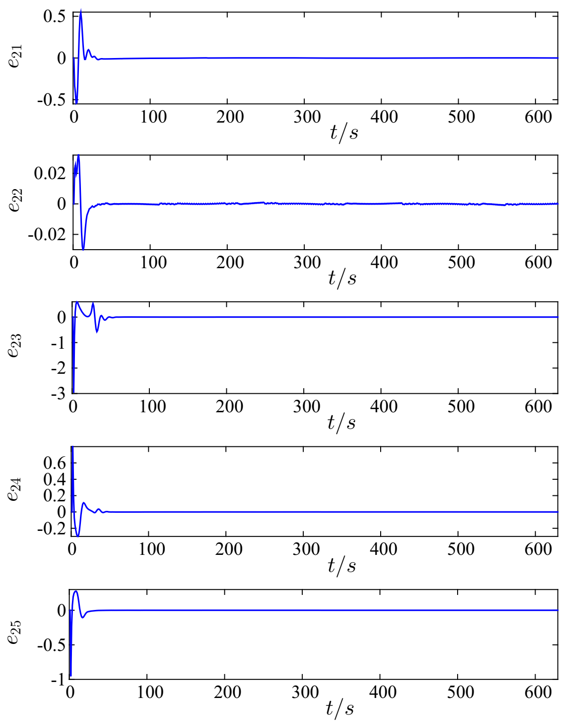

Fig. 6 Response of sliding variable $\boldsymbol{s}_1$

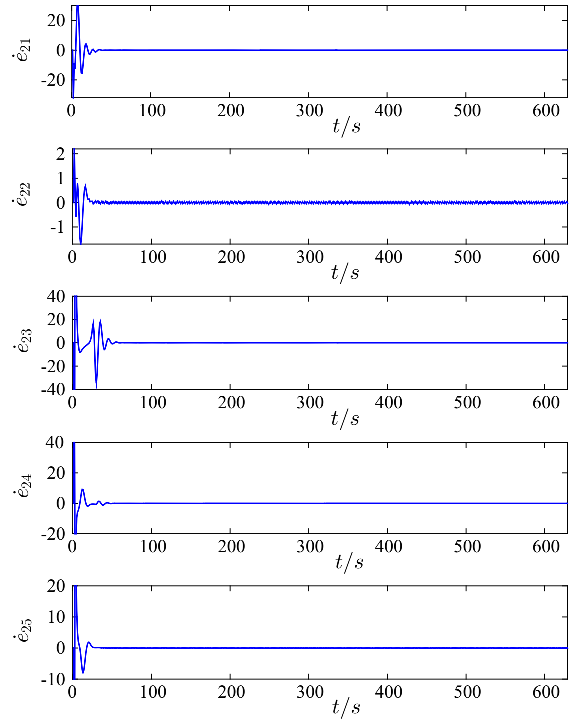

Fig. 7 Response of sliding variable $\boldsymbol{s}_2$

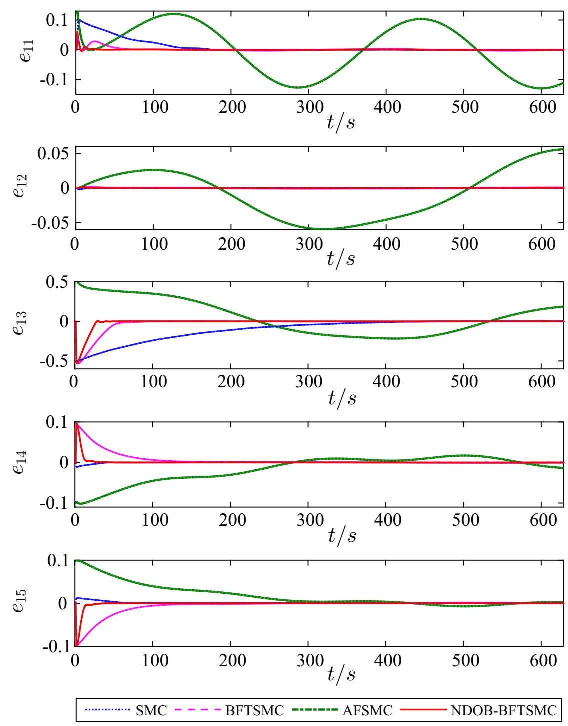

Fig. 8 Comparisons on the tracking error $\boldsymbol{e}_1$ among different schemes

Table 1 Performance comparison

Performance comparison	SMC	BFTSMC	AFSMC	NDOB-BFTSMC
Transient response	Fair	Good	Fair	Excellent
Steady-state error	Fair	Good	Fair	Excellent
IAE				
$e_{1,1}$	6.17896	1.81943	47.15735	0.54927
$e_{1,2}$	0.08343	0.42633	19.68233	0.10454
$e_{1,3}$	61.87908	15.16351	121.03432	7.2905
$e_{1,4}$	0.24909	3.76569	15.34152	0.68086
$e_{1,5}$	0.46998	3.98120	11.85191	0.71812
ISE				
$e_{1,1}$	0.35888	0.02260	4.52796	0.00641
$e_{1,2}$	0.00003	0.00035	0.81758	0.00003
$e_{1,3}$	16.81229	5.27161	31.73684	2.59959
$e_{1,4}$	0.00140	0.17486	0.76993	0.04092
$e_{1,5}$	0.00338	0.19674	0.57654	0.04398
RMSE				
$e_{1,1}$	0.02389	0.00599	0.08484	0.00319
$e_{1,2}$	0.00022	0.00075	0.03605	0.00022
$e_{1,3}$	0.16349	0.09155	0.22462	0.06429
$e_{1,4}$	0.00149	0.01667	0.03499	0.00807
$e_{1,5}$	0.00232	0.01769	0.03028	0.00836
Computational time (ms)	45.74	43.15	129.37	48.29
Lines of code	23	26	56	31

ence and actual trajectories of underwater vehicles in 3D and separate-dimension presentations, from which one can clearly observe that underwater vehicles are able to track the reference trajectory with high accuracy using the proposed NDOB-BFTSMC scheme, and a remarkable transient response of trajectory tracking can be obtained by the proposed control laws. The output of disturbance observer, namely, the estimate of the lumped disturbance, and the corresponding observation error of unknown lumped disturbance is shown in Figs. 3 and 4, respectively, which show that a remarkable estimation of the unknown lumped disturbance is achieved by using NDOB-BFTSMC. Figures 5, 6 and 7 show the responses of the sliding surface and the sliding variables, from which one can observe that the sliding surface is forced into a region of origin, namely, the system trajectories can be forced into the region of sliding surface $\boldsymbol{\sigma}$, and the validity is demonstrated by the convergence of sliding variables $\boldsymbol{s}_1$ and $\boldsymbol{s}_2$ in Figs. 6 and 7, respectively.

To verify the superiority of the proposed NDOB-BFTSMC scheme in terms of tracking accuracy, the comparisons with other schemes, i.e., SMC, BFTSMC, AFSMC, on the tracking error $\boldsymbol{e}_1$ are exhibited in Fig. 8, from which one can observe higher initial errors in the first 20 runs for the NDOB-BFTSMC scheme due to the high frequency disturbances, and then the robustness of the controller is enhanced along with the finite-time convergence stability. The responses of tracking errors can immediately reflect the transient responses of each control schemes such that the proposed control scheme can obtain better transient and steady-state responses by comparing with other control schemes in Fig. 8. Moreover, the comprehensive performance comparisons for tracking errors of the position and attitude of underwater vehicles are summarized in Table 1, where the integral time square error (IAE), i.e., $\text{IAE} = \int_0^t |e(\tau)|d\tau$, the integral square error (ISE), i.e., $\text{ISE} = \int_0^t e^2(\tau)d\tau$ and the root-mean-square error (RMSE), i.e., $\text{RMSE} = \left(\frac{1}{t}\int_0^t e^2(\tau)d\tau\right)^{1/2}$, are utilized to assess the transient and steady-state performance in trajectory tracking of underwater vehicles. For computational time of each scheme, we run each scheme ten times and take the average value as the computation time of the corresponding scheme. According to [43], theoretically, the computational time of the proposed NDOB-BFTSMC is higher than that of SMC and BFTSMC since there exists more online parameters in the proposed scheme. The theoretical analysis is demonstrated by computational time in Table 1, but there is only slight gaps with other schemes which is acceptable for practical application. Furthermore, the

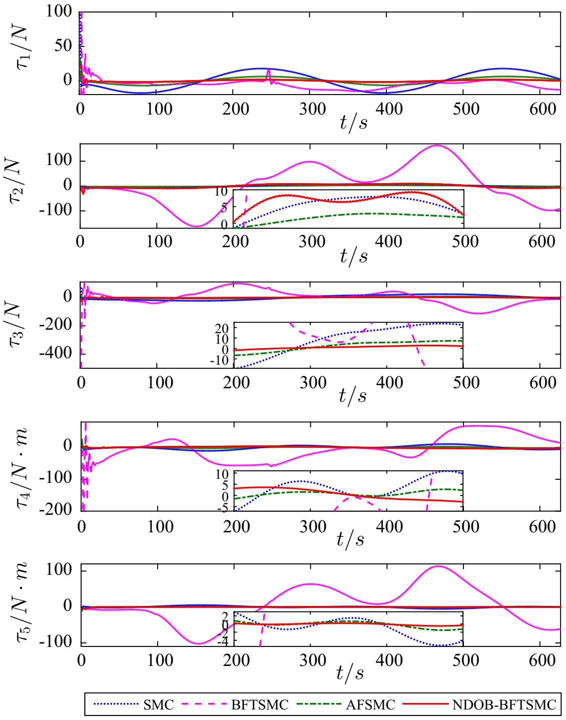

Fig. 9 Comparisons on control inputs $\boldsymbol{\tau}$ among different schemes

lines of code are used to assess the program complexity of each control scheme since the program complexity is an important fact for controller design in practice. From Table 1, it can be seen that the lines of code for the proposed NDOB-BFTSMC are larger than these of SMC and BFTSMC, but only slightly. In addition, the control inputs are shown in Fig. 9, from which one can see that the control inputs of the proposed NDOB-BFTSMC scheme are much smaller than these of BFTSMC and the chattering phenomenon is suppressed, which demonstrates that the effectiveness of the proposed NDO. From above simulation results, it is evident that the NDOB-BFTSMC scheme can provide improved robust performance with regard to system uncertainties and external disturbances.

5 Conclusion

In this paper, a novel backstepping finite-time sliding mode control scheme using nonlinear disturbance observer for trajectory tracking of the underwater vehicle system which suffers from system uncertainties and external disturbances. A robust output feedback control framework has been constructed by integrating backstepping design technique into the second-order sliding mode control such that the finite-time stability can be guaranteed. Under the control framework, by combining the system uncertainties and external disturbances into a single disturbance term, a nonlinear disturbance observer is employed to online identify the unknown lumped disturbance term. The stability of the overall closed-loop control system and the boundedness of the signals have been proved using the Lyapunov stability theorem, and the position and attitude tracking errors can be arbitrarily small by adjusting the designed parameters. From the comprehensive simulation results, the effectiveness and superiority of the proposed NDOB-BFTSMC scheme are indicated, such that the robust finite-time tracking performance of underwater vehicle systems with high-accuracy and rapid transient responses is obtained.

Acknowledgements The authors would like to thank Associate Editor and the reviewers for their very careful comments and helpful suggestions which improved this technical note significantly.
This work is supported by the National Natural Science Foundation of China (under Grants 51479018, 51379002 and 51009017) and Fundamental Research Funds for the Central Universities of China (under Grants 3132016335 and 3132016314).

References

1. Kuipers, M., Ioannou, P.: Multiple model adaptive control with mixing. IEEE Trans. Autom. Control **55**(8), 1822–1836 (2010)
2. Jiang, B., Gao, Z., Shi, P.: Adaptive fault-tolerant tracking control of near-space vehicle using Takagi–Sugeno fuzzy models. IEEE Trans. Fuzzy Syst. **18**(5), 1000–1007 (2010)
3. Peng, Z., Wang, D., Chen, Z.: Adaptive dynamic surface control for formations of autonomous surface vehicles with uncertain dynamics. IEEE Trans. Control Syst. Technol. **21**(2), 513–520 (2013)
4. Zhang, Y.P., Fidan, B., Loannou, P.A.: Backstepping control of linear time-varying systems with known and unknown parameters. IEEE Trans. Autom. Control **48**(11), 1908–1925 (2003)
5. Antonelli, G., Chiaverini, S., Sarkar, N., West, M.: Adaptive control of an autonomous underwater vehicle: experimental results on ODIN. IEEE Trans. Control Syst. Technol. **9**(5), 756–765 (2001)
6. Antonelli, G., Caccavale, F., Chiaverini, S.: A novel adaptive control law for underwater vehicles. IEEE Trans. Control Syst. Technol. **11**(2), 221–232 (2003)
7. Yoerger, D.N., Slotine, J.E.: Robust trajectory control of underwater vehicles. IEEE J. Ocean. Eng. **10**, 462–470 (1985)

8. Goheen, K., Jefferys, E.: Multivariable self-tuning autopilots for autonomous and remotely operated underwater vehicles. IEEE J. Ocean. Eng. **15**, 144–151 (1990)
9. Healey, A.J., Lienard, D.: Multivariable sliding mode control for autonomous diving and steering of unmanned underwater vehicles. IEEE J. Ocean. Eng. **18**, 327–339 (1993)
10. Lee, P.M., Hong, S.W., Lim, Y.K., Lee, C.M., Jeon, B.H., Park, J.W.: Discrete-time quasi-sliding mode control of an autonomous underwater vehicle. IEEE J. Ocean. Eng. **24**, 388–395 (1999)
11. McGookin, E.W.: Reconfigurable sliding mode control for submarine manoeuvring. In: Proceedings of the IEEE Oceans 01, pp. 1775–1782. Honolulu (2001)
12. Silvestre, Carlos: A bottom-following preview controller for autonomous underwater vehicles. IEEE Trans. Control Syst. Technol. **17**(2), 257–266 (2009)
13. Yang, Y., Ren, J.: Adaptive fuzzy robust tracking controller design via small gain approach and its application. IEEE Trans. Fuzzy Syst. **11**(6), 783–795 (2003)
14. Chen, B., Liu, X.P., Tong, S.C.: Adaptive fuzzy output tracking control of mimo nonlinear uncertain systems. IEEE Trans. Fuzzy Syst. **15**(2), 287–300 (2007)
15. Liu, Y.J., Wang, W., Tong, S.C., Liu, Y.S.: Robust adaptive tracking control for nonlinear systems based on bounds of fuzzy approximation parameters. IEEE Trans. Syst. Man Cybern. A Syst. Hum. **40**(1), 170–184 (2010)
16. Gao, Q., Feng, G., Wang, Y., Qiu, J.: Universal fuzzy models and universal fuzzy controllers for stochastic non-affine nonlinear systems. IEEE Trans. Fuzzy Syst. **21**(2), 328–341 (2013)
17. Luo, W., Soares, C.G., Zou, Z.: Neural-network, L_2-gain-based cascaded control of underwater robot thrust. IEEE J. Ocean. Eng. **39**, 630–640 (2014)
18. Chen, M., Ge, S.S., How, B.V.E.: Robust adaptive neural network control for a class of uncertain mimo nonlinear systems with input nonlinearities. IEEE Trans. Neural Netw. **21**(5), 796–812 (2010)
19. Liu, Y.J., Tong, S.C., Wang, D., Li, T.S., Chen, C.L.P.: Adaptive neural output feedback controller design with reduced-order observer for a class of uncertain nonlinear siso systems. IEEE Trans. Neural Netw. **22**(8), 1328–1334 (2011)
20. Polycarpou, M.: Stable adaptive neural control scheme for nonlinear systems. IEEE Trans. Autom. Control **41**(3), 447–451 (1996)
21. Gao, Y., Er, M.J.: Design for self-organizing fuzzy neural networks based on genetic algorithms. IEEE Trans. Fuzzy Syst. **11**(4), 462–477 (2003)
22. Chen, C.S.: Robust self-organizing neural-fuzzy control with uncertainty observer for mimo nonlinear systems. IEEE Trans. Fuzzy Syst. **19**(4), 694–706 (2011)
23. Wang, N., Er, M.J., Meng, X.: A fast and accurate online selforganizing scheme for parsimonious fuzzy neural networks. Neurocomputing **72**(16–18), 3818–3829 (2009)
24. Wang, N., Er, M.J., Meng, X., Li, X.: An online self-organizing scheme for parsimonious and accurate fuzzy neural networks. Int. J. Neural Syst. **20**(5), 389–403 (2010)
25. Wang, N.: A generalized ellipsoidal basis function based online selfconstructing fuzzy neural network. Neural Process. Lett. **34**(1), 13–37 (2011)
26. Man, Z., Paplinskiand, A., Wu, H.: A robust MIMO terminal sliding mode control for rigid robotic manipulators. IEEE Trans. Autom. Control **39**(12), 2464–2469 (1994)
27. Feng, F., Yu, X., Man, Z.: Non-singular terminal sliding mode control of rigid manipulators. Automatica **38**(12), 2159–2167 (2002)
28. Perruquetti, W., Barbot, J.P.: Sliding Mode Control in Engineering. Marcel-Dekker, New York (2002)
29. Edwards, C., Colet, E.F., Fridman, L.: Advances in variable structure and sliding mode control. Spfinger, Berlin (2006)
30. Damiano, A., Gatto, G.L., Marongiu, I.: Second-order sliding mode control of DC drives. IEEE Trans. Ind. Electron. **51**, 364–373 (2014)
31. Taheri, B., Case, D., Richer, E.: Force and stiffness backstepping-sliding mode controller for pneumatic cylinders. IEEE Trans. Mechatron. **19**(6), 1799–1809 (2014)
32. Chen, W.H.: Disturbance observer based control for nonlinear systems. IEEE/ASME Trans. Mechatron. **9**(4), 706–710 (2004)
33. Wu, J., Huang, J., Wang, Y., Xing, K.: Nonlinear disturbance observer-based dynamic surface control for trajectory tracking of pneumatic muscle system. IEEE Trans. Control Syst. Technol. **22**(2), 440–455 (2014)
34. Wei, X., Zhang, H., Guo, L.: Composite disturbance-observer-based control and terminal sliding mode control for uncertain structural systems. Int. J. Syst. Sci. **40**(10), 1009–1017 (2009)
35. Yang, J., Li, S., Yu, X.: Sliding-mode control for systems with mismatched uncertainties via a disturbance observer. IEEE Trans. Ind. Electron. **60**(1), 160–169 (2013)
36. Bu, X.W., Wu, X.Y., Chen, Y.X., Bai, R.Y.: Design of a class of new nonlinear disturbance observers based on tracking differentiators for uncertain dynamic systems. Int. J. Control Autom. Syst. **13**(3), 595–602 (2015)
37. Bu, X., Wu, X., Zhang, R., Ma, Z., Huang, J.: Tracking differentiator design for the robust backstepping control of a flexible air-breathing hypersonic vehicle. J. Frankl. Inst. **352**, 1739–1765 (2015)
38. Schoenwald, D.A.: Auvs: in space, air, water, and on the ground. IEEE Control Syst. Mag. **20**, 15–18 (2000)
39. Fossen, T.I.: Marine Control Systems: Guidance, Navigation, and Control of Ships, Rigs and Underwater Vehicles, Trondheim. Marine Cybernetics AS, Norway (2002)
40. Bhat, S.P., Bernstein, D.S.: Finite-time stability of continuous autonomous systems. SIAM J. Control Optim. **38**(3), 751–766 (2000)
41. Feng, F., Yu, X., Man, Z.: Non-singular terminal sliding mode control of rigid manipulators. Automatica **38**(12), 2159–2167 (2002)
42. Choi, J.K., Kond, H.: On fault-tolerant control of a hovering AUV with four horizontal and two vertical thrusters. In: Proceedings of the IEEE Oceans 10. Sydney (2010)
43. Bu, X., Wu, X., Huang, J.: A guaranteed transient performance-based adaptive neural control scheme with low-complexity computation for flexible air-breathing hypersonic vehicles. Nonlinear Dyn. **84**, 2175–2194 (2016)